TISSUE ENGINEERING: Part A
Volume 19, Numbers 15 and 16, 2013
© Mary Ann Liebert, Inc.
DOI: 10.1089/ten.tea.2012.0711

A Comparative Evaluation of Factors Influencing Osteoinductivity Among Scaffolds Designed for Bone Regeneration

Erin L. Hsu, PhD,[1,2] Jason H. Ghodasra, MS,[1] Amruta Ashtekar, MS,[1] Michael S. Nickoli, MD,[1] Sungsoo S. Lee, BS,[3] Samuel I. Stupp, PhD,[2–5] and Wellington K. Hsu, MD[1,2,6]

Due to differing compositions, synthetic scaffolds developed for bone regeneration vary widely in efficacy. To quantify the impact of such differences on osteoinductivity, numerous parameters were examined. Absorbable collagen sponge (ACS), three ceramic-based carriers (#1–3) of varying compositions, mineralized allograft chips, and an experimental phosphoserine-rich nanofiber scaffold [S(P) gel] were compared in their ability to promote cell adhesion, proliferation/survival, growth factor binding/release, and osteogenic gene expression. Human preosteoblasts were found to adhere most efficiently to the S(P) gel, and the growth/survival was greatest on the S(P) and ACS scaffolds, with minimal growth seen on the allograft and Ceramic #3. In bone morphogenetic protein-2 (BMP-2) binding/release assays, ACS demonstrated a burst release pattern, whereas the allograft and the ceramics inefficiently released BMP-2. The S(P) gel showed the most ideal rates of growth factor binding and release. QPCR analyses showed significant differences in the *CXCL12*, *CXCR4*, and *RANKL* transcripts among the cells grown on these various scaffolds. Although some scaffolds showed an advantage over others in individual parameters, the nanofiber gel appears to provide the optimal balance in the factors important to osteoinductivity evaluated here.

Introduction

Each year, an increasing number of orthopedic procedures utilize bone regenerative technologies.[1] Whether to repair fractures that have failed to heal, to replace bone in segmental bone defects, or to promote fusion across a diseased joint, these treatment modalities aim to overcome a variety of unfavorable conditions. Regenerative technologies can be tailored to optimize healing based on patient characteristics and risk factors, including osteoporosis, smoking, and immunodeficiency.

While a number of bone regenerative technologies are available for surgeons' use, delayed healing, pain, and nonunion are complications that continue to occur. Autogenous cancellous bone graft promotes both osteoinduction and osteoconduction, but has limited availability, and its use can be complicated by pain, blood loss, and scarring.[2–3] Although allogeneic bone graft avoids donor-site morbidity, its use is somewhat limited by immune-mediated rejection, potential disease transmission, and decreased osteogenic potential from sterilization procedures.[4]

Due to the efficacy and safety concerns associated with the use of bone grafts, a growing number of new treatment modalities have been investigated and utilized clinically. However, these new bone graft substitutes are not without their own challenges. Recombinant human bone morphogenetic protein-2 (rhBMP-2) in combination with an absorbable collagen sponge (ACS) requires a supraphysiologic dose that carries potential complications, including bone resorption, graft migration, hematoma formation, radiculitis, and heterotopic ossification.[5–11] Other growth factors, such as platelet-rich plasma, have shown a limited efficacy in promoting healing.[12] While some preclinical studies have investigated the potential of allogeneic mesenchymal stem cell (MSC) therapy, efficacy concerns have thus far prevented its introduction into clinical practice. Although many ceramic-based bone graft substitutes have proven safe, because their osteoinductive capability is limited, bone healing can be suboptimal.[13–15]

Shortcomings of current bone graft-substitute technologies have led to an extensive search for the optimal biomimetic scaffold.[1] Such a scaffold would not be limited in supply nor

[1]Department of Orthopaedic Surgery, Northwestern University, Chicago, Illinois.
[2]Institute for BioNanotechnology in Medicine, Northwestern University, Chicago, Illinois.
Departments of [3]Materials Science and Engineering, [4]Chemistry, [5]Medicine, and [6]Neurologic Surgery, Northwestern University, Chicago, Illinois.

carry a risk of immune-mediated rejection or disease transmission. However, the ability to create a microenvironment that mimics one or more of the natural states that occurs during the endogenous healing process would make such a scaffold truly appealing.[16] The ideal scaffold would not only provide the appropriate mechanical stability and allow bone growth throughout its structure (osteoconduction), but would also attract undifferentiated cells and induce them to proceed down the osteoblastic lineage (osteoinduction). Factors such as progenitor cell adhesion, survival, and proliferation are dependent on several components of the scaffold's architecture; porosity, surface area-to-volume ratio, pore interconnectivity, and surface texture impact these basic functions of progenitor cells, which in turn affect the osteoinductive capacity of the scaffold.

While biomimetic scaffolds have the potential to promote superior bone formation, little is known about the optimal composition and preparation characteristics that maximize a scaffold's osteoinductive properties. Nanoscaffolds are in theory more biocompatible than their microcounterparts due to an increased surface area, which allows for enhanced binding and interaction with progenitor cells and growth factors. Such scaffolds are also advantageous in that they can be tailored to bind particular growth factors deemed to provide an osteoinductive stimulus, thereby increasing bioactivity. A systemic comparative evaluation of various micro- and nanoscaffolds in their impact on factors influencing osteoinductive capacity could shed light on the components critical to osteoinductivity *in vivo*. In this study, we evaluated five clinically available scaffolds, as well as an experimental supramolecular peptide amphiphile (PA) nanofiber matrix were compared in their impact on osteoinductive factors such as progenitor cell adhesion and proliferation, growth factor sequestration, alkaline phosphatase (ALP) activity, and gene expression changes.

Materials and Methods

Scaffolds

Materials evaluated in this study vary in design and application, though they are used clinically for the purpose of bone regeneration and intended to elicit spinal fusion. For the sake of simplicity, however, the term "scaffold" is used in this study as a general reference to the collective materials, even though these products are not necessarily sold as scaffolds. We utilize this as a general term, as the intent of the study was to evaluate the materials for the ability to influence the factors critical for osteogenic differentiation and compare the commercially available materials with a nanogel scaffold that is not currently clinically available. Other than the nanogel scaffold, all materials selected are FDA-approved for human use, available at regional hospitals, and used commonly by orthopedic surgeons.

The first scaffold evaluated in this study was ACS (Medtronic Sofamor Danek, Memphis, TN), which is sold as a bone graft substitute intended to be used in combination with rhBMP-2 (INFUSE®; Table 1). It is noteworthy that ACS was used in this study without rhBMP-2, with the exception of the growth factor release assays. Ceramic #1 (3.5% Type I Collagen + 15% hydroxyapatite/85% β-tricalcium phosphate composite; Medtronic Sofamor Danek), Ceramic #2 (β-tricalcium phosphate; Synthes, West Chester, PA), and Ceramic #3 (20% Type I Collagen/80% β-tricalcium phosphate; Integra Orthobiologics, Irvine, CA) are all identified as Resorbable Calcium Salt Bone Void Filler FDA Class II devices. The mineralized, crushed allograft chips used in this study (AlloSource, St. Louis, MO) is a product regulated by the FDA under the category, Human Cells, Tissues, and Cellular and Tissue-based Products (HCT/Ps), and is also not sold commercially as a scaffold. The phosphoserine-containing PA [S(P)-PA] utilized in this study is experimental only (Fig. 1). The PA nanofiber matrix [abbreviated S(P) gel] was chosen, because the nanofibers present phosphoserine residues on their surface that promote hydroxyapatite mineralization with its c-axis parallel to the long axis of the nanofibers, mimicking the hierarchical structure of bone.[17,18] S(P)-PA molecules were synthesized using the standard 9-fluorenylmethoxycarbonyl (Fmoc) solid-phase peptide synthesis and purified by high-performance liquid chromatography as described previously.[18] The purified material was lyophilized and stored at −20°C until use. Equal volumes of S(P)-PA (2 wt%) and $CaCl_2$ (20 mM) were mixed to form entangled nanofiber gels.

Cell culture

MG-63 human preosteoblasts (ATCC, Manassas, VA) were grown in a minimal essential medium supplemented with 1% penicillin/streptomycin/Amphotericin B/10% FBS at 37°C /5% CO_2. Osteogenic conditions were defined as the MEM supplemented with 50 μg/mL ascorbic acid/10 mM β-glycerophosphate/10 nM dexamethasone.

Cell adhesion assays

Dry, uncompacted scaffolds were cut in a sterile hood using a thumb scalpel fitted with a number-11-style blade. ACS and

Table 1. Scaffold Compositions and Suppliers

Scaffold	*Composition*	*Commercial supplier*
Absorbable Collagen Sponge (ACS)	Type 1 Collagen	Medtronic Sofamor Danek (Danek, Memphis, TN)
Ceramic #1	3.5% Type I Collagen + 15% hydroxyapatite/85% β-tricalcium phosphate ceramic composite (96.5%)	Medtronic Sofamor Danek (Danek, Memphis, TN)
Ceramic #2	β-tricalcium phosphate (100%)	Synthes (West Chester, PA)
Allograft	Mineralized, crushed chips	Allosource (St. Louis, MO)
Ceramic #3	20% Type I collagen + 80% β-tricalcium phosphate	Integra Orthobiologics (Irvine, CA)
S(P) gel	phosphoserine-containing PA nanofiber gel, biodegradable	Currently experimental only

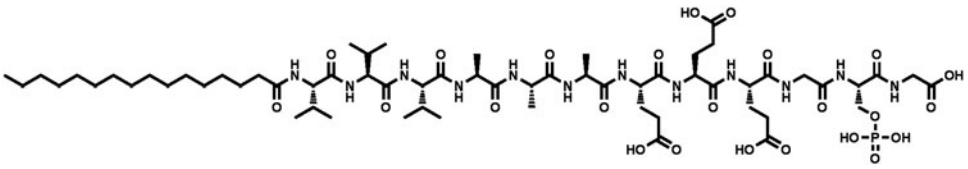

FIG. 1. ChemDraw structure depicting the phosphorylated serine [S(P)] peptide amphiphiles, with sequence: palmitoyl-VVVAAAEE-EGS(P)G (MW: 1435).

all ceramics were cut to an approximate volume of 0.064 cm^3 (4×4×4 mm for ceramics #1 and 3; 3.5×4.3×4.3 mm for ACS and ceramic #2) using digital microcalipers with a resolution of 0.01 mm. Allograft chips measuring ~2-mm thick were collected to cover the surface area of two wells of a standard 96-well plate (0.0317-cm^3 surface area). After measurements, the scaffolds were placed in quadruplicate into individual wells of an ultra-low-binding 96-well plate, and 2×10^3 MG-63 cells suspended in 50 μL of osteogenic medium were seeded onto each scaffold. In the case of the S(P) gel, a 25 μL of a 2wt% S(P)-PA solution was overlaid into the bottom of each well. A 23 μL suspension of 2×10^3 cells in the osteogenic medium was spiked with 2 μL of 250 mM $CaCl_2$, and that suspension was inoculated directly into each PA solution (final [$CaCl_2$] of 10 mM). For all scaffolds, cells were allowed to adhere (and S(P) gel allowed to assemble) for 20 min before the wells were overlaid with 175 μL of osteogenic medium. After 2 h, the overlaying medium was removed, and the scaffolds were washed twice with PBS. All microscaffolds were removed in their entirety with forceps and placed into sterile microfuge tubes, where they were digested with 300 μL of 100 nM proteinase K (Amresco, Solon, OH) at 60°C overnight. For the S(P) gel wells, proteinase K was added directly to the wells after removal of the medium. With a pipette tip, the gels were resuspended in the proteinase K solution, transferred to microfuge tubes, and digested overnight with the dry scaffolds. The following day, all digests were centrifuged at 16,000 *g* for 10 min, and 5 μL of each supernatant was stained in triplicate with picogreen (Invitrogen, Carlsbad, CA) and read on a SpectraMax M5 absorbance reader at A405 at the Northwestern University Institute for Nanotechnology in Medicine (IBNAM) core facility. A standard curve was used to correlate absorbance with DNA content.

Cell proliferation assays

Proliferation/survival studies were performed similarly to adhesion assays in replicates of 4, with slight variations; 1×10^3 cells were inoculated onto each scaffold in a total volume of 50 μL and allowed to incubate for 20 min before overlay of the osteogenic medium. Scaffolds were not washed before harvest. At increasing time points out to 14 days, scaffolds were harvested as described under the section Cell adhesion assays, and DNA was quantitated via picogreen staining as described above.

BMP-2 binding/release assays

Dry scaffolds measuring 0.135 cm^3 were placed into microfuge tubes and preloaded with 0.5 μg of recombinant human BMP-2. An equivalent volume of S(P) gel was assembled as described above, with 0.5 μg of recombinant human BMP-2 in place of the cells/osteogenic medium. All scaffolds were allowed to adsorb growth factor for 20 min, after which time 700 μL of release medium (0.1% BSA/PBS) was gently applied to each tube. Tubes were pulse-spun, and immediately thereafter, 300 μL of release medium was removed from each tube. An additional 300 μL of fresh release medium was again overlaid, and the tubes were pulse-spun. The second 300 μL aliquot of release medium was removed from each tube and was combined with the original aliquot to obtain the day-0 samples. A second aliquot of 300 μL of fresh release medium was applied to each tube, and scaffolds were incubated at 4°C. At increasing time points out to 28 days, the same procedure was applied, with two aliquots of release medium removed and fresh medium subsequently replaced and stored for future analysis. All aliquots were frozen at −80°C until growth factor quantitation. BMP-2 was quantitated using a sandwich ELISA (R&D Systems, Minneapolis, MN).

ALP activity assays

Scaffolds measuring 0.064 cm^3 were inoculated with 1×10^3 cells in an osteogenic medium as described under the section Cell proliferation assays and grown for 8 days, with one change of medium on day 4. On day 8, supernatants were removed and stored at −80°C until analysis. Scaffolds were removed from wells and placed into microfuge tubes for lysis. The S(P) gels were lysed directly in the plate. All scaffolds were lysed at room temperature for 10 min with frequent vortexing, after which time the lysates were removed to a new microfuge tube and spun at 2500 *g* for 10 min at 4°C. The supernatants were collected and stored at −80°C until use. ALP activity was quantitated using a colorimetric assay according to the manufacturer's instructions (Anaspec, Fremont, CA). A405 was read on a SpectraMax M5 absorbance reader at the Northwestern University IBNAM core facility.

Gene expression analyses

Five×10^5 cells were resuspended in the osteogenic medium and seeded onto scaffolds measuring 1 cm^3 in 12-well plates. S(P) gels of equivalent size were assembled as described above. Twenty-four hr after inoculation, dry scaffolds were removed from the plate, and RNA was harvested using a combination of Trizol Reagent® (Invitrogen) and RNEasy MinElute RNA cleanup kit (Qiagen, Valencia, CA) using a protocol modified from the manufacturers' instructions. The S(P) gels were digested directly in the plate, and then processed identically to dry scaffolds. Briefly, 1 mL Trizol® was added to each scaffold-containing tube. Scaffolds were vortexed for 15 s and incubated at room temperature for 5 min, with frequent vortexing. Two hundred μL of chloroform was then added to each tube, followed by 15-s vortex, 1-min incubation, and a final 15-s vortex. Tubes were then spun at 15,000 *g* for 10 min. The top layer was removed to a fresh tube containing 700 μL of buffer RLT/β-mercaptoethanol (RNEasy MinElute kit). Five hundred μL of 100% ethanol was added to each tube and vortexed. Samples were applied to the MinElute spin columns, spun at 15,000 *g*, and collection tubes decanted.

Table 2. Primer and Probe Sequences

Gene		Sequence
CXCR4	Forward	AGCAGGTAGCAAAGTGACG
	Reverse	CCTCGGTGTAGTTATCTGAAGTG
	Probe	FAM-TACTGATCCCCTCCATGGT AACCGC-IABkFQ
RANKL	Forward	ATCACAGCACATCAGAGCAG
	Reverse	GAGGACAGACTCACTTTATGGG
	Probe	HEX-TGGATGGCTCATGGTTAGA TCTGGC-IABkFQ
GAPDH	Forward	CAGCCTCAAGATCATCAGCAA
	Reverse	GGCCATCCACAGTCTTCTG
	Probe	HEX-ATGACCACAGTCCATGCC ATCACT-IABkFQ

This process was repeated until the full volume was applied to the membrane. Columns were washed with buffer RPE and 80% DEPC ethanol as instructed by the manufacturer. RNAs were eluted in 30 μL of DEPC water and quantitated using a Qubit fluorimeter and corresponding RNA quantitation kit (Invitrogen). cDNAs were transcribed using the QuantiTect Reverse Transcription kit (Qiagen) as instructed. Gene expression analyses were performed via TaqMan QPCR (PerfecTa® QPCR Supermix; Quanta Biosciences, Gaithersberg, MD). The *CXCR4* transcripts were normalized to *β-Actin* and *GAPDH*. Primer and probe sequences are described in Table 2 (Integrated DNA Technologies, Coralville, IA). The β-Actin and CXCL12 primer/probe sets were purchased from Applied Biosystems (Foster City, CA; sequences proprietary).

Statistical analyses

All measurements were performed in replicates of 3–5 in three independent experiments. Where indicated, the results are expressed as mean ± standard deviation. For comparison between groups, a two-tailed Student's *t*-test was used, where probability *p*-values < 0.05 were considered statistically significant.

Results

Variable adhesion rates among scaffolds

Cell adhesion studies were performed to compare the ability of preosteoblasts to adhere to the various scaffolds, which exhibit vastly differing surface properties. Adhesion rates varied widely among the scaffolds (Fig. 2). The cells were sequestered most efficiently by the S(P) gel, demonstrating the advantage of cell encapsulation upon gel assembly [$p < 0.01$ S(P) gel vs. allograft; $p < 0.001$ S(P) gel vs. all other groups]. Allograft chips and ACS also showed a significantly greater ability to adhere cells relative to all three ceramics ($p < 0.001$ allograft vs. each of the ceramics; $p < 0.01$ ACS vs. Ceramic #3, $p < 0.001$ ACS vs. Ceramic #s 1 and 2). The three ceramic-based scaffolds showed a relatively little capacity to sequester cells 2 h postinoculation. The trending increase in cellular adhesion to allograft relative to ACS was not statistically significant.

Proliferation/survival rates of cells grown on scaffolds

Survival/proliferation of preosteoblasts was evaluated over 14 days. Similar to adhesion studies, the S(P) gels contained the greatest amount of DNA 2 h postinoculation (deemed day 0, Fig. 3). In contrast, the three ceramics contained nearly undetectable amounts of DNA at day 0. At day 3, ACS showed the capacity for significant cell expansion, whereas the cell number was unchanged in the S(P) gel. In contrast, the amount of DNA present on allograft decreased from day 0 to day 3, indicating that cell survival was negatively impacted by inoculation onto this scaffold. All three ceramics again showed very little DNA content on day 3. By day 7, Ceramic #s 1 and 2 showed increased DNA content, demonstrating that the few cells that adhered initially to those scaffolds were indeed able to survive and proliferate. This trend followed out to day 14, although the exponential growth seen on Ceramic #2 leveled off after day 10. Notably, 1 of the 3 trials showed no growth of MG-63 cells on Ceramic #2 (data not shown). This was presumably because the number of cells that successfully adhered to that scaffold was insufficient for survival. Both Ceramic #1 and ACS still showed cells in the exponential growth phase at day 14. Cells grown on the S(P) gel showed a more modest degree of expansion that continued through day 14. On the other hand, little-to-no DNA was detectable on allograft and Ceramic #3 scaffolds, even on day 14.

BMP-2 sequestration and release

To evaluate the capacity of each scaffold to bind and release growth factor *ex vivo*, recombinant human BMP-2 was

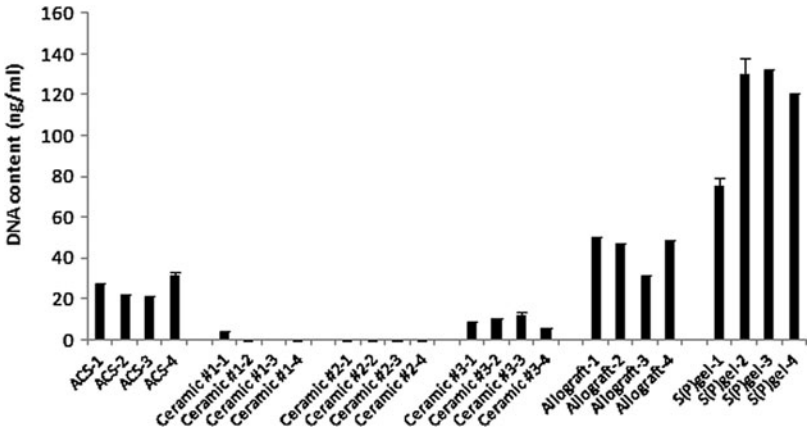

FIG. 2. Adhesion rates among scaffolds. Cells were inoculated onto scaffolds and allowed to adhere for 2 h at 37°C /5% CO_2, after which time the scaffolds were washed twice with PBS and digested with proteinase K. The lysates were stained with picogreen to quantitate DNA. $p < 0.01$ S(P) gel versus allograft; $p < 0.001$ S(P) gel versus all other groups; $p < 0.001$ allograft versus each of the three ceramics; $p < 0.01$ ACS versus Ceramic #3, $p < 0.001$ ACS versus Ceramic #s 1 and 2. Data are representative of three independent experiments.

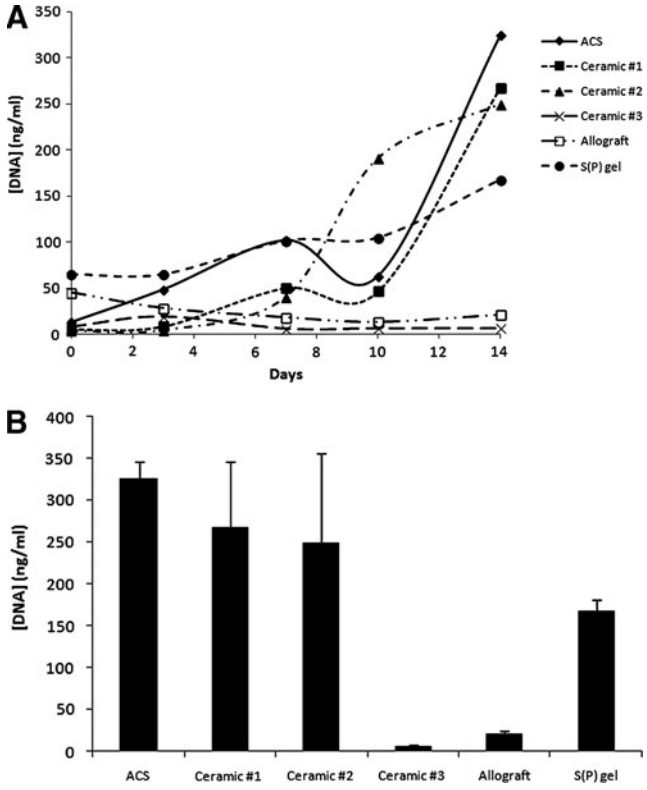

FIG. 3. Proliferation/survival rates among scaffolds. Cells were inoculated in an osteogenic medium onto scaffolds and incubated for increasing time points out to 14 days **(A)**. Day-0 time point was taken 2 h postinoculation. At each time point, the scaffolds were removed from wells, digested, and the DNA stained with picogreen. Day-14 data points are depicted separately to show standard deviations, providing a view of typical variability **(B)**. Data are representative of three independent experiments.

preloaded onto scaffolds, and at increasing time points, the release medium was harvested and evaluated for BMP-2 content. Allograft bound the BMP-2 least efficiently, followed by ACS and Ceramic #2 (Fig. 4). ACS performed uniquely in this assay, demonstrating a burst release of growth factor over the first several days, followed by a more continual release pattern over the 28 days. In contrast, the S(P) gel bound the growth factor far more efficiently at the initial loading and released BMP-2 over the remainder of the 28 days in a consistent manner. The remaining scaffolds inefficiently released BMP-2, as is evident from the flat slopes of their release curves.

ALP activity in preosteoblasts grown on various scaffolds

ALP activity was measured in both lysates and supernatants from cells grown on scaffolds for 8 days in osteogenic conditions. ALP detected in the cell supernatants was mildly, but significantly, reduced in Ceramic #1 and allograft groups relative to all others (Fig. 5A; $p < 0.05$). On the other hand, ALP activity was lowest in the lysates of cells grown on ACS and allograft. The S(P) gel groups showed similar ALP activity to the ceramic-based scaffold groups, and was only significantly elevated ($p < 0.05$) relative to the ACS and allograft groups (Fig. 5B). ALP levels in cells grown on Ceramic #s 1 and 2 were significantly elevated over those on ACS, and the levels of ALP were also significantly elevated in the cells grown on Ceramic #2 relative to allograft ($p < 0.05$).

Gene expression changes in preosteoblasts grown on various scaffolds

Several gene transcripts influential in osteogenic differentiation were quantitated in preosteoblasts seeded onto the various scaffolds. Significant differences were seen in expression levels of *CXCL12*, a chemokine recently shown to be required for BMP-2-mediated osteogenic differentiation.[19] The highest levels of *CXCL12* were seen in the cells grown on the S(P) gel, with elevated levels also seen in cells grown on ACS (Fig. 6A). The three ceramic-based scaffolds showed relatively low *CXCL12* levels. Notably, insufficient quantities of RNA were harvested from cells grown on allograft 24 h after seeding, and the transcripts were therefore not quantitated in such samples. The receptor for CXCL12, CXCR4, was also quantitated, and preosteoblasts grown on the S(P) gel expressed *CXCR4* at levels 5–10-fold higher than other scaffolds (Fig. 6B). Interestingly, cells grown on Ceramic #2 showed increased *RANKL* expression relatively to all other scaffolds (Fig. 6C). No reproducible significant differences

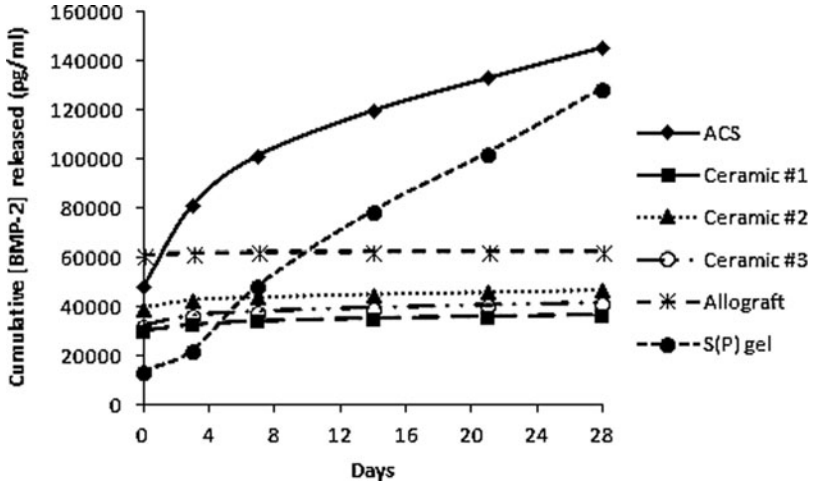

FIG. 4. Growth factor binding/release assays. Equivalently sized scaffolds (0.135 cm^3) were loaded with 500 ng BMP-2, and overlaid with the release medium. At increasing time points out to 28 days, media were harvested and stored for subsequent growth factor quantitation via ELISA. Data represent cumulative growth factor release, where a flat slope indicates no further release.

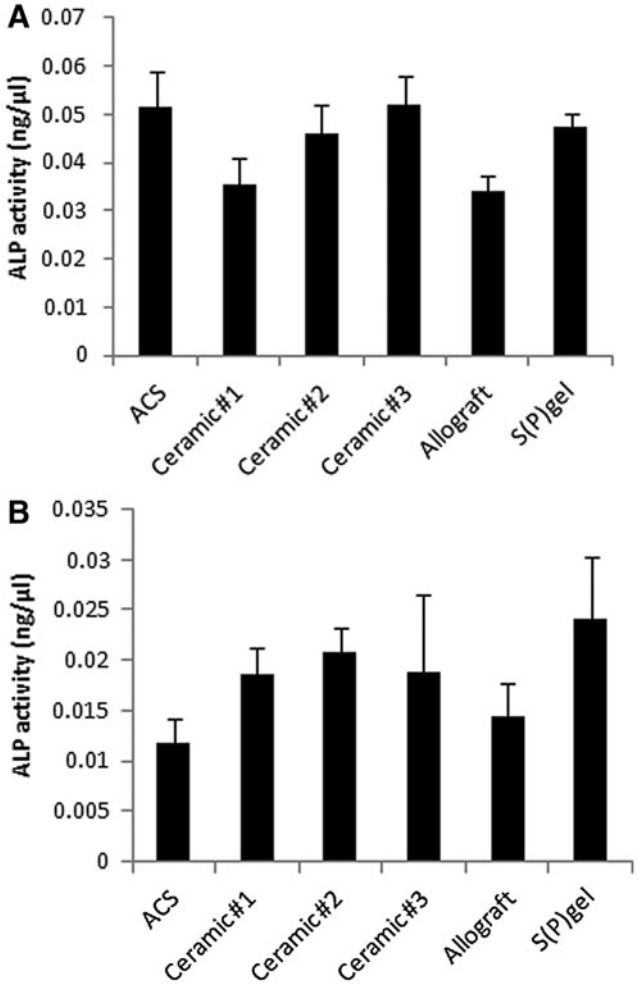

FIG. 5. Alkaline phosphatase (ALP) activity. Cells were inoculated in an osteogenic medium onto scaffolds and incubated for 8 days. The medium was replaced on day 4, and on day 8, was collected for quantitation of ALP activity in the supernatants **(A)**. Cells were then lysed on scaffolds for the quantitation of membrane-bound ALP **(B)**.

were seen in *Runx2*, *ALP*, or osteocalcin transcripts (data not shown).

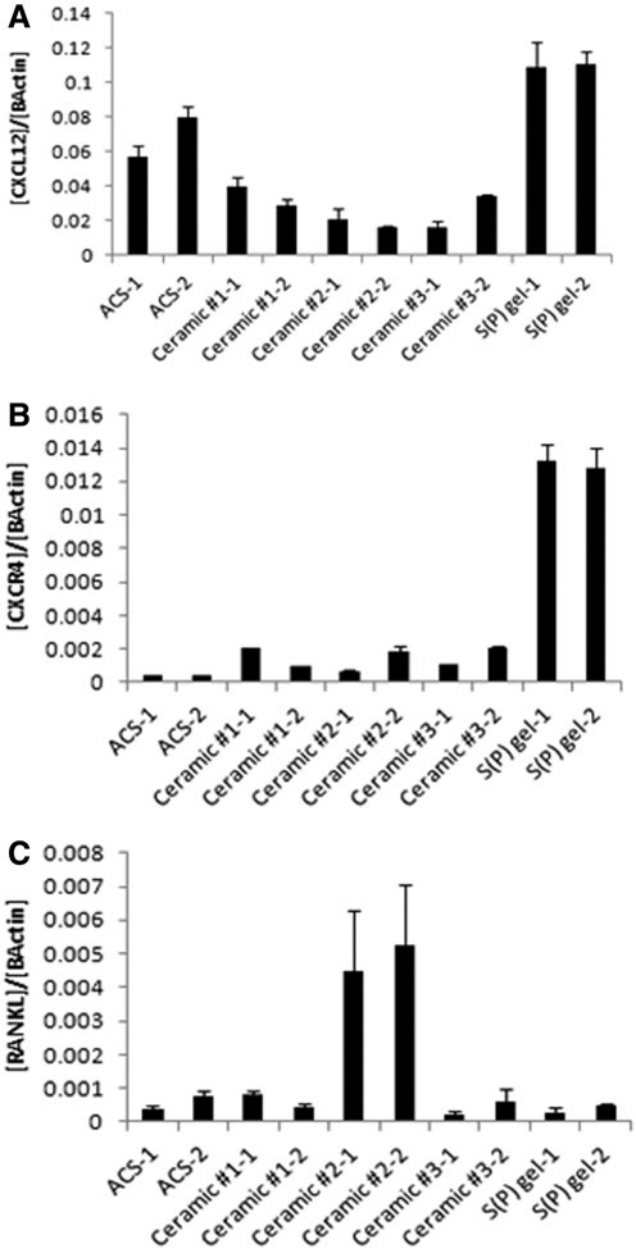

FIG. 6. Gene expression changes. MG-63 preosteoblasts were seeded onto scaffolds and incubated in the osteogenic medium for 24 h. *CXCL12* **(A)**, *CXCR4* **(B)**, and *RANKL* **(C)** mRNAs were quantitated via TaqMan QPCR. Data were normalized to β-Actin.

Discussion

An array of diverse factors likely impacts the success rate of bone graft substitutes. In general, it is reasonable to assume that a scaffold that allows for a high rate of preosteoblast adhesion and also promotes cell survival and proliferation would more actively facilitate osteoinductivity and bone regeneration. After implantation, it is necessary for the material to adsorb plasma constituents and connective tissue, followed by recruitment of progenitor cells that will terminally differentiate into mature osteoblasts.[20] Since cellular adhesion is a major contributor to the compatibility of a biomaterial, we evaluated the capacity of scaffolds to promote adhesion of preosteoblasts in this study. Because nanoscaffolds have an increased surface area and improved osteointegrative properties, it is unsurprising that the PA nanofiber gel utilized in this study—which encapsulates cells upon assembly—performed superior to other scaffolds in promoting cell adhesion.

Overall, ACS and the S(P) gel demonstrated the best balance between the capacity to adhere preosteoblasts and promote their survival and growth. These scaffolds therefore have an apparent advantage in promoting a cell-friendly environment relative to other comparable products. Ceramic #s 1 and 2 provided an environment facilitating substantial growth, despite poor initial adhesion rates. In contrast, Ceramic #3 showed no promotion of cell survival/growth. Since cells did not adhere efficiently to this ceramic, the lack of DNA content on time points subsequent to day 0 could

also be a result of the poor adhesion rate to that scaffold. This difference in performance may be partially explained by their respective differences in composition; Ceramic #1 contains added hydroxyapatite, and both Ceramics 1 and 3 contain type I collagen (3.5% and 20%, respectively), but Ceramic #2 has neither. Based on the success of Ceramic #2 in our proliferation assays, hydroxyapatite is likely not a required component for cell growth/survival on a ceramic. Since the ACS group shows clearly that type I collagen promotes cell growth/survival, it is likely that the preparation methods for Ceramic #3 somehow influenced its capacity to maintain cell survival and promote growth. As a result, that ceramic may not perform well clinically as a bone graft substitute when compared to other scaffolds.

Seebach *et al.* found that Tutoplast®—a mineralized human cancellous allograft processed through five proprietary steps (Tutoplast process: delipidation, osmotic contrast treatment, oxidation, dehydration, and irradiation)—promoted cell growth out to 10 days, a result our allograft data did not corroborate.[21] This discrepancy could be explained by differences in the method of allograft preparation, but could also be a result of the different method of cell quantitation; this group utilized the MTT assay as an indirect measure of cell number, whereas we have found MTT results to inaccurately reflect the number of cells grown on scaffolds (data not shown). Instead, we used DNA quantitation as a direct measure of cell number. Although allograft was also a clear promoter of cell adhesion in our studies, it did not support the survival and proliferation of preosteoblasts.

The mineralized allograft utilized in this study performed the worst in BMP-2 binding/release studies, with a minimal binding capacity and a subsequent poor release rate from the scaffold. Similarly, after initial inoculation of BMP-2 onto the various scaffolds, the three ceramics released almost no BMP-2, as depicted by slopes near zero (Fig. 4). Considering that progenitor cells are chemotactic for BMP-2, this lack of propensity to release growth factor is a clear disadvantage in promoting bone regeneration.[22] The poor ability of allograft and the ceramics to release growth factor should therefore be taken into account in choosing a bone graft substitute. Although ACS demonstrated a relatively poor capacity to initially bind BMP-2, its capacity for growth factor release was greater than all other scaffolds tested, as is evident by the steep slope of the release curve (Fig. 4). This response is in line with the classic burst release of BMP-2 associated with the clinical use of INFUSE.[23] This effect likely renders ACS unable to ensure longer-term growth factor delivery and has been postulated to contribute to the adverse effects associated with the use of rhBMP-2/ACS clinically.[24–26]

Relative to all other scaffolds, the S(P) gel showed a superior rate of initial growth factor binding, followed by a steady and sustainable release over the period studied. In comparing ACS and the S(P) gel, it is important to note that in a rat spinal arthrodesis model, we have observed ACS to be completely degraded by day 7, whereas the S(P) gel is biodegraded by approximately day 21 *in vivo* (data not shown). Therefore, the burst release before day 7 seen in the ACS group is likely greatly enhanced when rhBMP-2/ACS is utilized *in vivo,* which could lead to a pronounced host response. Since the rate of degradation of the S(P) gel is approximately threefold lower than that of ACS, the corresponding increase in slope of that release curve would be more moderate *in vivo*.

The differences in the ALP levels among groups *in vitro* were minor. Indeed, we did not see reproducible changes in the *ALP* transcripts among cells grown on the different scaffolds (data not shown). The significant changes seen in expression levels of the chemokine, *CXCL12*, and its receptor, *CXCR4*, could very well influence the osteoinductive capacity of a particular scaffold. The CXCR4/CXCL12 axis promotes human bone marrow MSC growth and survival, and CXCL12-overexpressing bone marrow MSC have been shown to form increased levels of ectopic bone *in vivo*.[27] CXCL12 is also required for BMP-2-mediated osteogenic differentiation of both C2C12 cells and primary MSC, influencing OCN synthesis, ALP activity, and expression of Runx2, Osx, and Dlx5 pro-osteogenic transcription factors.[19] Importantly, the interaction between CXCL12 and CXCR4 is required for the homing of MSC to the sites of bone healing.[28,29] Wynn *et al.* observed that MSC migrate toward a CXCL12 gradient in a dose-dependent manner.[30] With such a multifactorial impact, the expression levels of both *CXCL12* and *CXCR4* are therefore highly relevant to osteogenesis, and increased levels would be considered a strong advantage of one scaffold over another. The elevated levels of *CXCL12* in cells grown on the S(P) gel and, to a lesser extent, ACS could feasibly provide such cells with a greater capacity for survival and growth, as we saw in this study.[26] Even more striking was the significant increase of *CXCR4* expression in cells grown on the S(P) gel relative to all other scaffolds. Interestingly, the levels of *CXCR4* were lowest in the ACS group, with cells in the S(P) gel group expressing over 25-fold greater levels of *CXCR4*. Taken together, the S(P) gel scaffold provided the most advantageous expression profile for *CXCL12/CXCR4*, and it is reasonable to expect that such a relative induction would provide that scaffold with an increased capacity for both recruitment of preosteoblasts/MSC to the site of injury as well as promotion of the osteogenic lineage.[19,31–32] On the other hand, the levels of *RANKL—a* critical factor in osteoclastogenesis—were significantly higher in cells grown on Ceramic #2 relative to other scaffolds. If reproducible *in vivo,* such elevated levels of *RANKL* would be concerning for a scaffold designed to promote bone formation.

A notable limitation to this study is the fact that the allograft utilized here was mineralized, and demineralized allograft would likely have promoted cell survival/growth and factor sequestration in a more effectual manner. However, the physical and handling properties of demineralized bone matrices (DBMs) provided significant logistical challenges in performing adhesion assays with this type of scaffold, thereby precluding their comparative evaluation in this study. The ability to include DBMs may have shed light on whether distinct processing protocols negatively influence the ability of nondemineralized allograft to retain and release BMPs. The information gleaned from these data must also be considered in the context that ours represents an *in vitro study,* and as described above, the performance of each scaffold *in vivo*—gene expression changes in particular—may be further influenced by complicating factors unique to such an environment.

Surgeons are offered a host of options for bone grafting, yet few *in vitro* studies have directly compared these products for their capacity to influence individual factors critical for osteoinduction. Of the three principles governing the process of

osteoinduction—cell recruitment, cell differentiation, and bone formation—the first two can be evaluated, at least preliminarily, using *in vitro* techniques.[33] This study evaluates the factors that impact the first two of these principles and represents an initial approach to the characterization of scaffolds for bone regeneration. Our results provide an insight into the response of human preosteoblasts and growth factors to such scaffolds, and therefore a basis for deciding which scaffolds warrant further investigation. Together with follow-up studies, this work could explain the clinical performance of such scaffolds and provide physicians with information on which may promote osteogenic differentiation most effectively.

Acknowledgments

This work was supported in part by the NIH National Institute for Dental and Craniofacial Research (NIDCR) [5R01DE015920-07]. S.S.L. is supported by Samsung Scholarship Foundation graduate fellowship.

Disclosure Statement

WK Hsu consults for Stryker, Zimmer, Medtronic, Pioneer Surgical, and Graftys, has received institutional/research support from Medtronic, Baxter, and Pioneer Surgical, and serves on the boards of AAOS, RMEC, and LSRS. EL Hsu declares the same conflicts. SI Stupp consults for Royal DSM, NV, and owns stock in Nanotope. The remaining authors have no conflicts of interest to declare.

References

1. Dawson, J.I., and Oreffo, R.O. Bridging the regeneration gap: stem cells, biomaterials and clinical translation in bone tissue engineering. Arch Biochem Biophys **473,** 124, 2008.
2. Dimar, J.R., 2nd, Glassman, S.D., Burkus, J.K., *et al.* Clinical and radiographic analysis of an optimized rhBMP-2 formulation as an autograft replacement in posterolateral lumbar spine arthrodesis. J Bone Joint Surg Am **91,** 1377, 2009.
3. Summers, B.N., and Eisenstein, S.M. Donor site pain from the ilium. A complication of lumbar spine fusion. J Bone Joint Surg Br **71,** 677, 1989.
4. Barriga, A., Díaz-de-Rada, P., Barroso, J.L., *et al.* Frozen cancellous bone allografts: positive cultures of implanted grafts in posterior fusions of the spine. Eur Spine J **13,** 152, 2004.
5. Brower, R.S., and Vickroy, N.M. A case of psoas ossification from the use of BMP-2 for posterolateral fusion at L4-L5. Spine **33,** E653, 2008.
6. McClellan, J.W., Mulconrey, D.S., Forbes, R.J., *et al.* Vertebral bone resorption after transforaminal lumbar interbody fusion with bone morphogenetic protein (rhBMP-2). J Spinal Disord Tech **19,** 483, 2006.
7. Muchow, R.D., Hsu, W.K., and Anderson, P.A. Histopathologic inflammatory response induced by recombinant bone morphogenetic protein-2 causing radiculopathy after transforaminal lumbar interbody fusion. Spine J **10,** E1, 2010.
8. Pradhan, B.B., Bae, H.W., Dawson, E.G., *et al.* Graft resorption with the use of bone morphogenetic protein: lessons from anterior lumbar interbody fusion using femoral ring allografts and recombinant human bone morphogenetic protein-2. Spine **31,** E277, 2006.
9. Vaidya, R. Transforaminal interbody fusion and the "off label" use of recombinant human bone morphogenetic protein-2. Spine J **9,** 667, 2009.
10. Vaidya, R., Sethi, A., Bartol, S., *et al.* Complications in the use of rhBMP-2 in PEEK cages for interbody spinal fusions. J Spinal Disord Tech **21,** 557, 2008.
11. Wong, D.A., Kumar, A. Jatana, S., *et al.* Neurologic impairment from ectopic bone in the lumbar canal: a potential complication of off-label PLIF/TLIF use of bone morphogenetic protein-2 (BMP-2). Spine J **8,** 1011, 2008.
12. Sys, J., Weyler, J., Van Der Zijden, T., *et al.* Platelet-rich plasma in mono-segmental posterior lumbar interbody fusion. Eur Spine J **20,** 1650, 2011.
13. Jenis, L.G., and Banco, R.J. Efficacy of silicate-substituted calcium phosphate ceramic in posterolateral instrumented lumbar fusion. Spine **35,** E1058, 2010.
14. Epstein, N. An analysis of noninstrumented posterolateral lumbar fusions performed in predominantly geriatric patients using lamina autograft and beta tricalcium phosphate. Spine J **8,** 882, 2008.
15. Brandoff, J.F., Silber, J.S., and Vaccaro, A.R. Contemporary alternatives to synthetic bone grafts for spine surgery. Am J Orthop **37,** 410, 2008.
16. Willie, B.M., Petersen, A., Schmidt-Bleek, K., *et al.* Designing biomimetic scaffolds for bone regeneration: why aim for a copy of mature tissue properties if nature uses a different approach. Soft Matter **6,** 4976, 2010.
17. Hartgerink, J.D., Beniash, E., and Stupp, S.I. Self-assembly and mineralization of peptide-amphiphile nanofibers. Science **294,** 1684, 2001.
18. Mata, A., Geng, Y., Henrikson, K.J., Aparicio, C., *et al.* Bone regeneration mediated by biomimetic mineralization of a nanofiber matrix. Biomaterials **31,** 6004, 2010.
19. Zhu, W., Boachie-Adhei, O., Rawlins, B.A., *et al.* A novel regulatory role for stromal derived factor-1signaling in bone morphogenetic protein-2 osteogenic differentiation of mesenchymal C2C12 cells. J Biol Chem **282,** 18676, 2007.
20. Biggs, M.J.P., Richards, R.G., Gadegaard, N., *et al.* Interactions with nanoscale topography: Adhesion quantification and signal transduction in cells of osteogenic and multipotent lineage. J Biomed Mater Res Part A **91A,** 195, 2008.
21. Seebach, C., Schultheiss, J., Wilhelm, K., *et al.* Comparison of six bone-graft substitutes regarding to cell seeding efficiency, metabolism and growth behaviour of human mesenchymal stem cells (MSC) *in vitro.* Injury **41,** 731, 2010.
22. Fiedler, J., Röderer, G., Günther, K.P., *et al.* BMP-2, BMP-4, and PDGF-bb stimulate chemotactic migration of primary human mesenchymal progenitor cells. J Cell Biochem **87,** 305, 2002.
23. King, W.J., and Krebsbach, P.H. Growth factor delivery: How surface interactions modulate release *in vitro* and *in vivo.* Adv Drug Deliv Rev **64,** 1239, 2012.
24. Takahashi, Y., Yamamoto, M., and Tabata, Y. Enhanced osteoinduction by controlled release of bone morphogenetic protein-2 from biodegradable sponge composed of gelatin and b-tricalcium phosphate. Biomaterials **26,** 4856, 2005.
25. Helm, G.A., Sheehan, J.M., Sheehan, J.P., *et al.* Utilization of type I collagen gel, demineralized bone matrix, and bone morphogenetic protein-2 to enhance autologous bone lumbar spinal fusion. J Neurosurg **86,** 93, 1997.
26. Zhang, S., Doschak, M.R., and Uludag, H. Pharmacokinetics and bone formation by BMP-2 entrapped in polyethyleniminecoated albumin nanoparticles. Biomaterials **30,** 5143, 2009.
27. Kortesidis, A., Zannettino, A., Isenmann, S., *et al.* Stromal-derived factor-1 promotes growth, survival, and development

of human bone marrow stromal stem cells. Blood **105,** 3793, 2005.
28. Fong, E.L.S., Chan, C.K., and Goodman, S.B. Stem cell homing in musculoskeletal injury. Biomaterials **32,** 395, 2011.
29. Granero-Molto, F., Weis, J.A., Miga, M.I., *et al.* Regenerative effects of transplanted mesenchymal stem cells in fracture healing. Stem Cells **27,** 1887, 2009.
30. Wynn, R.F., Hart, C.A., Corradi-Perini, C., *et al.* A small proportion of mesenchymal stem cells strongly expresses functionally active CXCR4 receptor capable of promoting migration to bone marrow. Blood **104,** 2643, 2004.
31. Hosogane, N., Huang, Z., Rawlins, B.A., *et al.* Stromal derived factor-1 regulates bone morphogenetic protein 2-induced osteogenic differentiation of primary mesenchymal stem cells. Int J Biochem Cell Biol **42,** 1132, 2010.
32. Kitaori, T., Ito, H., Schwarz, E.M., *et al.* Stromal cell-derived factor 1/CXCR4 signaling is critical for the recruitment of mesenchymal stem cells to the fracture site during skeletal repair in a mouse model. Arthritis Rheum **60,** 813, 2009.
33. Miron, R.J., and Zhang, Y.F. Osteoinduction: a review of old concepts with new standards. J Dental Res **91,** 736, 2012.

Address correspondence to:
Erin L. Hsu, PhD
Department of Orthopaedic Surgery
Northwestern University
676 N. St. Clair St., Ste 1350
Chicago, IL 60611

E-mail: erinkhsu@gmail.com

Received: November 30, 2012
Accepted: March 6, 2013
Online Publication Date: May 1, 2013